Progressive DNA Bending Is Made Possible by Gradual Changes in the Torsion Angle of the Glycosyl Bond

Leonardo Pardo,*# Nina Pastor,* and Harel Weinstein*

*Department of Physiology and Biophysics, Mount Sinai School of Medicine, New York, New York 10029 USA, and #Laboratorio de Medicina Computacional, Unidad de Bioestadística, Facultad de Medicina, Universidad Autónoma de Barcelona, 08193 Bellaterra, Barcelona, Spain

ABSTRACT Structural comparisons have led to the suggestion that the conformational rearrangement that would be required to change A-DNA into the TA-DNA form of DNA observed in the complex with the TATA box binding protein (TBP) could be completed by modifying only the value of the glycosyl bond χ by ~45°. The lack of a high number of crystal structures of this type makes it difficult to conclude whether a smooth transition from A-DNA to TA-DNA can occur without disrupting at any point either the Watson-Crick base pairing or the A-DNA conformation of the backbone. To explore the possibility of such a smooth transition, constrained molecular dynamics simulations were carried out for the double-stranded dodecamer d(GGTATATAAAAC), in which a transition from A-DNA to TA-DNA was induced by modifying only the χ angle values. The results demonstrate the feasibility of a continuous path in the A-DNA to TA-DNA transition. Varying extents of DNA curvature are also attainable, by maintaining the A-DNA backbone structure and Watson-Crick hydrogen bonding while changing the χ angle value smoothly from that in A-DNA to one corresponding to B-DNA.

INTRODUCTION

The formation of a complex between the TATA box binding protein (TBP) and the TATA box of the core promoter is a crucial event in the initiation of transcription of protein-coding genes by RNA polymerase II (Pol II) (Burley and Roeder, 1996; Pugh, 1996). The three-dimensional structure of the TBP/DNA complex (Geiger et al., 1996; Juo et al., 1996; Kim et al., 1993a,b; Kosa et al., 1997; Nikolov et al., 1995, 1996; Tan et al., 1996) reveals that TBP recognizes the minor groove of the TATA element. In contrast to TBP, which undergoes only a small conformational change upon binding, the 8-bp TATA box is clearly unwound and dramatically bent toward the major groove (see Lebrun and Lavery, 1997, for a review on unusual DNA conformations). When flanked by standard B-DNA conformation, this novel TATA box structure produces a major change in the trajectory of the DNA, corresponding to a junction-type bend of ~90° (Kim et al., 1993a,b). This bend is absolutely required for TFIIB recruitment at the promoter (Choy and Green, 1993; Kosa et al., 1997; Nikolov et al., 1995) and transcription by Pol II. Two mechanisms have been proposed to produce the bend in DNA by TBP: the low dielectric environment of the protein increases the repulsion between the phosphates across the minor groove, causing the bend toward the major groove (Elcock and McCammon, 1996); alternatively, the stretching of the backbone of the DNA produces a structure reminiscent of the one found in the complex with TBP (Lebrun et al., 1997).

Statistical analysis of various conformational parameters of the DNA in the complex showed that the torsion angles of the TATA box in the complex with TBP (TA-DNA) resemble those of the A-DNA structure, with the exception of the glycosyl-bond torsion angle (χ: O4′-C1-N1-C2 for pyrimidines and O4′-C1-N9-C4 for purines), which is in the range typical for B-DNA (Guzikevich Guerstein and Shakked, 1996). This particular combination of backbone dihedral angles produces a very strong inclination of the base pairs with respect to the helical axis (Olson, 1977), and is responsible for the 90° bend seen in the context of B-DNA, where the base pairs have zero inclination. The structural comparisons by Guzikevich et al. (1996) thus led to the suggestion that the transition from A-DNA to the TA-DNA conformation in the complex could be completed by modifying only the value of χ by ~45° (Guzikevich et al., 1996). Inspection of the crystal structure of the TATA box complex with TBP (Kim et al., 1993a,b) further suggested that the intercalation of two pairs of conserved Phe residues into the first two and last two base pairs of the TATA box may be sufficient to produce the desirable change in χ. However, Guzikevich et al. (1996) pointed out that the lack of a high number of crystal structures of this type makes it difficult to propose a smooth transition from A-DNA to TA-DNA without the disruption of either the Watson-Crick base pairing or the A-DNA conformation of the backbone. It remained unclear, therefore, whether a continuous mechanism is possible in which a gradual change in the rotation around χ would produce a gradual change in the DNA trajectory. Because resolving this uncertainty could lead to insights into the actual mechanism of DNA bending by TBP, we have used molecular dynamics simulations of the TATA box-containing dodecamer

Received for publication 27 March 1997 and in final form 10 February 1998.

Address reprint requests to Dr. Harel Weinstein, Department of Physiology and Biophysics, Mount Sinai School of Medicine, One Gustave L. Levy Place, Box 1218, New York, NY 10029-6574. Tel.: 212-241-7018; Fax: 212-860-3369; E-mail: hweinstein@inka.mssm.edu.

0006-3495/98/05/2191/08 $2.00

d(GGTATATAAAAC) to explore the feasibility of a continuous path in the A-DNA to TA-DNA transition solely by changing the χ angle values, and within the constraints of an A-DNA backbone and Watson-Crick base pairing.

METHODS

The A-DNA to TA-DNA conformational transition

The double-stranded DNA dodecamer d(GG**TATATA-AA**AC) that contains the consensus TATA box sequence TATAt/aAt/aX (in bold), was built in the canonical A-DNA conformation (Arnott and Hukins, 1972), a common starting point for simulations with the AMBER package (Cheatham and Kollman, 1996; Cieplak et al., 1997). To achieve electroneutrality of the system, counterions (a total of 22 sodium ions) were included, positioned initially at a distance of 5 Å from each P atom. The DNA and the counterions were placed in a rectangular box containing Monte Carlo-equilibrated TIP3P water (3987 water molecules). The molecular dynamics simulations were run with the Sander module of AMBER 4.1 (Pearlman et al., 1995), in the all-atom force field (Cornell et al., 1995), SHAKE bond constraints, with a 2-fs time step, and at a constant temperature of 300 K coupled to a heat bath. Initially, the DNA atoms were kept fixed, whereas the sodium ions and water molecules were heated (from 0 to 300 K in 15 ps) and equilibrated (from 15 to 100 ps) at constant pressure with isotropic scaling. The final box sizes after equilibration were ~68.0 Å by 41.9 Å by 44.7 Å, resulting in a final density of 1.04 g cm^{-3}. Subsequently, the whole system was energy minimized (500 steps), heated (from 0 to 300 K in 15 ps), and equilibrated (from 15 to 50 ps), and the production run (from 50 to 250 ps) was carried out at constant volume, using the particle mesh Ewald (PME) method to evaluate electrostatic interactions (Darden et al., 1993). The PME charge grid spacing was ~1.0 Å, the B-spline interpolation order was 4, and the charge grid was interpolated with the direct sum tolerance set to 0.00001, common parameters for PME simulations with the AMBER package (Cheatham and Kollman, 1996).

Flat harmonic restraints (32 kcal mol^{-1} rad^{-1}) were applied during the entire simulation to maintain the A-DNA conformation by constraining the torsional angles α, β, γ, δ, ϵ, and ζ of the 24 nucleotides of the dodecamer, and the torsional angle χ (206 ± 5°) of the four nucleotides at both ends of the DNA helix (see Table 1). In addition, flat harmonic restraints (32 kcal mol^{-1} $Å^{-1}$) were also applied to maintain Watson-Crick base pairing (within ±0.1 Å) in all basepairs.

The values of χ for the 16 nucleotides comprising the TATA box were changed in the following manner. During the first 50 ps, the torsional angles χ were kept close to the standard A-DNA values (206 ± 5°) with harmonic restraints of 32 kcal mol^{-1} rad^{-1}. For the next 150 ps, the values of χ were simultaneously and slowly changed from those obtained during the A-DNA trajectory to those obtained in the crystal structure (Kim et al., 1993a) of the TA-DNA conformation (listed in Table 2), with harmonic restraints of 64 kcal mol^{-1} rad^{-1}. Finally, for the last 50 ps of the simulation, the values of χ were kept close to the TA-DNA values obtained in the crystal structure with flat harmonic restraints of 32 kcal mol^{-1} rad^{-1}. It is important to note that the four nucleotides at both ends of the DNA helix are kept within the A-DNA conformation during the entire simulation. The average and standard deviation of the restraint energy that maintains the A-DNA conformation are 65.3 kcal/mol and 8.8 kcal/mol, respectively, during the first 50 ps. The restraint energies that maintain the A-DNA conformation of the backbone and change the χ angle are even smaller during the A-DNA to TA-DNA transition (the next 150 ps): 53.8 kcal/mol and 6.3 kcal/mol for the average and standard deviation, respectively. Finally, during the last 50 ps of simulation, the average and standard deviation of the restraing energy (keeping the TA-DNA conformation) are also of the same magnitude: 56.8 kcal/mol and 7.1 kcal/mol. Judging from the fact that the values for the dihedral angle β lie outside the flat restraint interval zone, this dihedral angle might be responsible for most of the restraint energy.

Progressive DNA bending

The mechanism of DNA bending by gradual changes in the torsion angle of the glycosyl bond is illustrated by the

TABLE 1 Backbone dihedral angles: restraint zones and canonical structures

Dihedral angle	r1	r2	r3	r4	A-DNA AMBER	A-DNA GG&S	TA-DNA GG&S
α	261.0	271.0	281.0	291.0	276.0	301.0	294.0
β	193.0	203.0	213.0	223.0	208.0	172.0	172.0
γ	30.0	40.0	50.0	60.0	45.0	42.0	52.0
δ	69.0	79.0	89.0	99.0	84.0	79.0	96.0
ϵ	164.0	174.0	184.0	194.0	179.0	215.0	205.0
ζ	296.0	306.0	316.0	326.0	311.0	282.0	274.0
χ	191.0	201.0	211.0	221.0	206.0	201.0	245.0

Between r1 and r2, and between r3 and r4, the force constant is 32 kcal mol^{-1} rad^{-1}: between r2 and r3 there is no restraining force. A-DNA AMBER: starting configuration in the simulation (Arnott and Hukins, 1972). A-DNA GG&S: canonical A-DNA backbone values from Guzikevich et al. (1996). TA-DNA GG&S: average TA-DNA backbone values derived by Guzikevich et al. (1996).

TABLE 2 Backbone dihedral angles for the TATA box

Base	δ	ϵ	ζ	α	β	γ	χ	phase	A
Sense strand: 5′ to 3′									
3-T	80.5	180.9	302.6	275.2	201.6	48.2	201.2	25.1	39.4
	83.4	219.8	263.4	50.5	160.4	299.2	198.8	34.6	41.1
4-A	87.2	185.8	308.7	274.4	198.3	47.7	235.2	10.1	34.1
	159.0	194.0	259.1	270.1	184.1	49.5	238.1	196.1	34.1
5-T	81.5	179.8	301.1	277.6	200.7	48.8	231.5	27.4	36.1
	80.1	192.8	279.2	286.7	177.2	52.9	231.2	63.6	48.4
6-A	88.9	184.8	305.9	277.4	202.9	48.2	259.3	0.6	33.2
	99.5	200.1	287.4	276.7	175.6	50.5	258.1	41.0	23.0
7-T	83.5	178.7	301.0	276.1	200.5	49.6	259.6	17.5	32.7
	78.0	178.2	270.4	296.6	167.2	54.5	263.2	49.2	46.2
8-A	88.1	183.7	304.6	274.7	196.0	49.5	252.4	359.7	32.9
	100.9	191.7	290.5	287.6	172.0	54.2	251.7	351.6	24.9
9-A	89.1	179.0	303.6	278.0	197.5	51.8	253.4	357.0	32.8
	95.4	214.0	290.7	286.6	177.1	56.1	253.4	20.4	27.4
10-A	89.9	181.9	308.2	272.5	194.7	49.5	274.1	357.0	34.3
	154.3	235.5	179.1	283.8	159.4	55.8	277.0	163.1	47.1
*	79.0	174.0	306.0	271.0	203.0	40.0			
	89.0	184.0	316.0	281.0	213.0	50.0			
Antisense strand: 3′ to 5′									
22-A	93.0	178.5	303.3	275.0	197.8	51.0	257.0	2.9	32.4
	150.5	197.0	279.0	277.4	185.5	66.5	258.8	153.2	50.5
21-T	88.9	178.6	302.8	277.3	195.1	50.8	245.3	12.7	30.6
	85.2	199.0	305.7	293.5	174.2	51.1	246.1	57.3	43.7
20-A	84.6	184.3	303.7	274.6	198.0	46.7	246.3	7.1	35.0
	82.2	200.4	258.0	305.9	141.7	49.8	248.4	10.3	46.0
19-T	84.7	181.1	305.5	276.5	202.9	50.0	243.3	18.9	33.7
	77.5	198.5	287.9	269.5	170.3	65.7	245.7	50.0	50.0
18-A	90.6	181.8	302.4	275.8	197.2	49.4	254.4	355.8	32.7
	85.8	189.7	277.3	300.9	157.9	44.8	253.4	41.6	43.0
17-T	84.2	181.5	303.4	275.9	199.3	47.9	239.4	22.3	33.4
	80.0	185.6	280.0	277.5	170.0	47.0	238.2	55.1	47.8
16-T	85.0	179.2	303.3	274.2	199.0	47.9	241.0	22.5	33.5
	105.0	198.3	276.4	283.0	173.9	64.1	243.4	103.7	34.7
15-T	83.3	185.0	305.3	278.9	200.1	50.4	229.4	32.6	34.6
	93.6	203.5	254.7	298.5	148.9	56.5	231.7	94.7	53.2
*	79.0	174.0	306.0	271.0	203.0	40.0			
	89.0	184.0	316.0	281.0	213.0	50.0			

A, Sugar pucker amplitude; *, flat harmonic restraint zero penalty interval. Above: final structure (average over 200–250 ps); below: target structure (Kim et al., 1993b; refined at 2.5 Å).

structures of d(GG**TATATAAA**AC) computed during the A-DNA to TA-DNA conformational transition (see previous section), at 50 ps, 150 ps, and the average structure computed from the simulation between 200 and 250 ps (Fig. 5). To emphasize the structural consequences of the structural transition, the DNA oligomers were extended at the 5′ and 3′ ends by substituting the original A-DNA regions d(GG) and d(AC) for double-stranded DNA d(GGGGGGGGG) and d(ACCCCCCCC) in the A-DNA conformation (Arnott and Hukins, 1972), respectively. The resulting structures show the transition from a straight A-DNA structure to an A/TA/A structure with two junctions. To compare the final structure obtained for the TATA box with the existing crystal structures of TBP/TATA box complexes, the average structure for the TATA box computed from the simulation between 200 and 250 ps was extended at the 5′ end by d(TGTATGTA) in the B-DNA conformation found outside the TATA box in the crystal structure of the complex with TBP and TFIIA (Geiger et al., 1996), and at the 3′ end by d(GGCTG) in the B-DNA conformation found outside the TATA box in the crystal structure of the complex with TBP and TFIIB (Nikolov et al., 1995). The addition of B/TA/B junctions is illustrated in Fig. 5 (see Results).

RESULTS AND DISCUSSION

A- to TA-conformational transition

The gradual change in the values of the χ angle throughout the molecular dynamics simulation is shown in Fig. 1 *A* for each nucleotide on the coding strand of the TATA box. Fig. 1 *B* shows the corresponding comparison of various structures, expressed as the root mean square difference (RMSD)

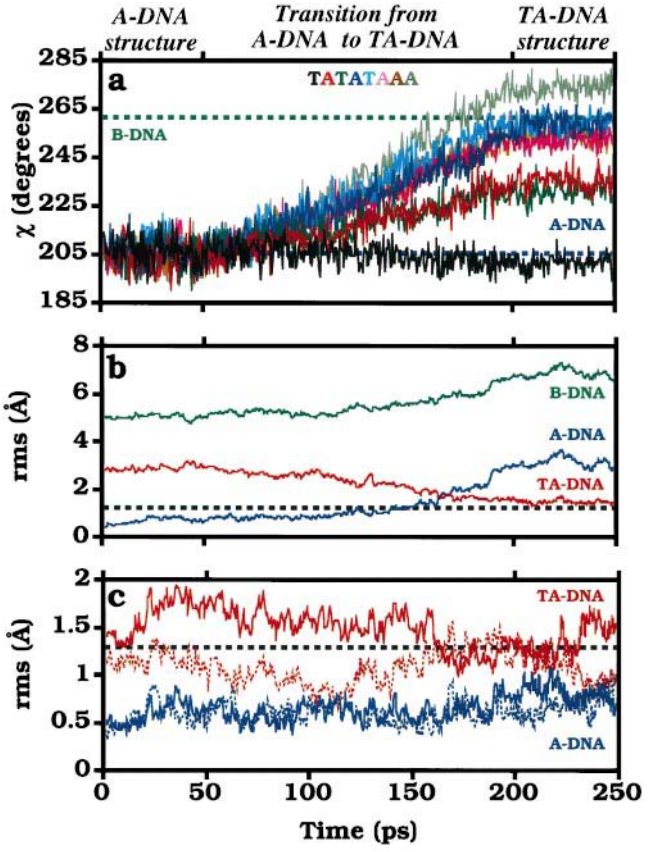

FIGURE 1 (*A*)Values of the glycosyl-bond torsional angle (χ) for each of the eight nucleotides (color coded individually in the figure) of the TATATAAA sequence in the TATA box, shown as a function of time. The χ angles of the other nucleotides in the dodecamer are not shown. During the 0–50-ps period of the simulation, the values of χ were restrained close to those in canonical A-DNA (*blue broken line*). Subsequently (during the 50–200-ps period), χ values were slowly changed to those found in the TA-DNA structure, and were maintained close to those in the TA-DNA structure during the 200–250-ps period (see Methods for details). The χ angles of the TA-DNA structure in the TBP complex (Kim et al., 1993a) are in the range of 231°-277°, with the exception of the angle corresponding to the first nucleotide of the TATA box (T), which remains close to the A-DNA value (199°, see *black line*). (*B*) RMSD comparison of the computer-simulated structures, canonical A-DNA (*blue*) and B-DNA (*green*), and the crystal structure of TA-DNA (*red*). Values are calculated for the heavy atoms of the 8-bp TATA box. The expected minimum RMSD between the computer-simulated structures and the crystal structure of TA-DNA, derived from *C*, is shown as a broken black line. (*C*) RMSD comparison of the coding strand A (*solid line*) and noncoding strand B (*broken line*) of the sugar-phosphate backbone, in the computer-simulated structures, compared to canonical A-DNA (*blue*), and to the crystal structure of TA-DNA (*red*). Each strand was matched separately.

in their atomic coordinates. The compared structures include the snapshots from the computer simulation, canonical A-DNA and B-DNA (Arnott and Hukins, 1972), and a crystal structure of TA-DNA (Kim et al., 1993a). The RMSD values indicate that as the simulation progresses and the χ angle values slowly change from those in A-DNA to those in the TA-DNA structure (Fig. 1 *A*), the computed structure gradually becomes more similar to the conformation found in the crystal structure of the TBP/TATA box complex (Fig. 1 *B*). At the end of the simulation, the average structure converged to the expected RMS difference of 1.3 Å from the crystal structure of TA-DNA (shown as a *black broken line* in Fig. 1 *B*). This RMSD of 1.3 Å is expected because it is the average of the RMS values between canonical A-DNA and TA-DNA backbones, calculated from the separate superpositions of the backbone in each strand (see *black broken line* in Fig. 1 *C*). The RMSD between computed and TA-DNA backbones (*red lines* in Fig. 1 *C*) is in the range of 1.0–1.9 Å for the coding strand A, and 0.6–1.6 Å for the noncoding strand B, with an average value of 1.3 Å (see *broken black line*). These small RMSD values confirm the proposed similarity, but not the identity, of the backbones of the A-DNA and the TA-DNA structures (Guzikevich et al., 1996), summarized in Table 2. Because of the application of restraints keeping the backbone in the A-DNA conformation during the simulation (see Methods and the *blue lines* in Fig. 1 *C*), this RMSD of 1.3 Å is in fact the minimum value that can be achieved from the comparison of the computed structures with the experimental TA-DNA, as long as the A-DNA constraints are in place (*broken black line* in Fig. 1 *B*).

A stereo view of the RMS best fit of the crystal structure of TA-DNA and the average structure computed from the simulation between 200 and 250 ps is shown in Fig. 2. Notably, the constrained simulation we have performed does not, in itself, ensure the convergence to this final structure. The process would fail if the path defined by changing only the χ angle value were incompatible with the constraints defined by the hypothesis of Guzikevich et al. (1996). As a matter of fact, omission of the H-bond constraints results in a slipped structure, as predicted by Olson (1977) and illustrated by Guzikevich et al. in figure 3 of their paper (Guzikevich et al., 1996).

As a further characterization of the relation between the final structure and the crystal structure of TA-DNA, selected geometrical parameters for the base pairs of the resultant TATA box are compared with A-DNA and with the target crystal structure in Fig. 3. Keeping in mind that the backbone was not allowed to relax in the simulation, it is remarkable to note the coincidence in the patterns for *inclination* (Fig. 3 *A*), *twist* (Fig. 3 *B*), and *slide* (Fig. 3 *C*) between the actual crystal structure (Kim et al., 1993a) and the average structure for the interval between 200 and 250 ps. On the other hand, the pattern for *roll* (Fig. 3 *D*) is not reproduced entirely, and *rise* (not shown) is not reproduced at all. A likely explanation for this failure is the discrepancy between the canonical A-DNA backbone dihedral angles (the ones used in AMBER or the ones listed by Guzikevich et al., summarized in Table 1) and the actual crystal structure backbone dihedral angles at the first and last base pair steps of the TATA box, identifiable in Table 2 (nucleotides 3, 4, 9, 10, 15, 16, 21, and 22). As indicated in table 1 of Guzikevich et al. (1996), these values, which deviate largely from the mean values found for the other base pairs of the TATA box, were excluded from their calculations of average values for the backbone dihedral angles of TA-DNA.

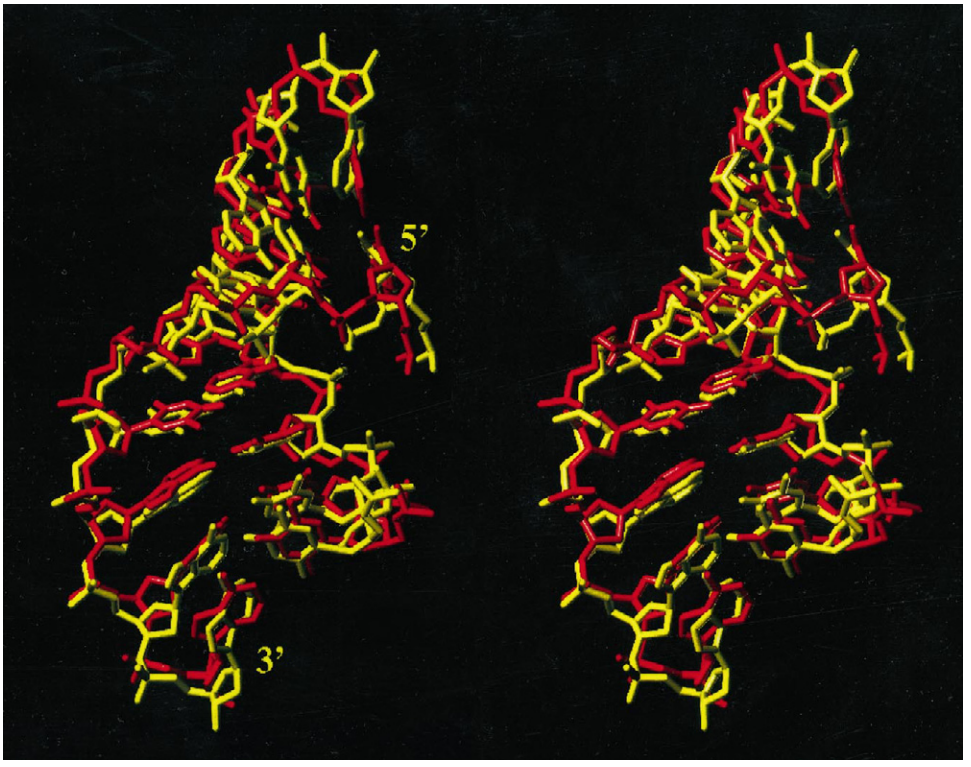

FIGURE 2 Stereo view of the RMS best fit of the average structure computed from the trajectory between 200 and 250 ps (*yellow*) and the DNA molecule of the TBP/TATA box crystal structure (Kim et al., 1993a) (*red*). Only the heavy atoms of the 8-bp TATA box are shown.

A striking feature of the transition from A-DNA to TA-DNA is illustrated in Fig. 4, which shows that the structural rearrangement is achieved by shifting the sugar-phosphate backbone of one strand by one residue relative to the complementary strand. This apparent shift of the strands relative to one another results in the characteristic change in orientation of the base pair observed before (Guzikevich et al., 1996; Olson, 1977). To illustrate the key phenomenon of gradual transformation from the A-DNA to the TA-DNA form, Fig. 4 depicts the structures of the central base pair T7:A18 of the TATA box obtained at 50 ps, 100 ps, 150 ps, and the average structure computed from the simulation in the 200–250-ps period. The comparison of the evolving structures brings into evidence the repositioning of the sugar moiety of A18 toward the 3′ end, and the progressive change in the orientation of the base pair with respect to the helix axis as a function of gradual χ change expressed in the simulation time. Thus the results illustrate the gradual change in the rotation around the χ angle during the simulation (Fig. 1 *A*), which brings about a gradual change in the inclination in the base pair through the continuous shift of the sugar-phosphate backbone (Fig. 4). In the absence of H-bond constraints between the base pairs, the change in χ results in the disruption of the base pair, as described by Olson (1977); hence one plausible role for the phenylalanine residues that partially intercalate into the DNA might be to guarantee that the base pairs do not slip.

Progressive DNA bending

The process of progressive DNA bending by the changes in the torsion angle of the glycosyl bond is illustrated in Fig. 5, which shows the structures computed during the A-DNA to TA-DNA conformational transition at 50 ps (*red*), 150 ps (*orange*), and the average structure computed from the trajectory between 200 and 250 ps (*yellow*), with the extensions at the 5′ and 3′ ends by DNA moieties in the A-DNA conformation (see second part of Methods, under Progressive DNA Bending). The computed structures of the TATA box during the conformational transition are shown as flat ribbons, whereas the extended atoms are shown as tube ribbons. The common extended atoms, at the 5′ end (*green*), were superimposed. The computed intermediates corresponding to structures with intermediate χ values exhibit different extents of DNA curvature (cf. the structure at 150 ps in *orange*) that are transitional between the starting point (the structure at 50 ps, in *red*, which according to Fig. 1 is still A-DNA) and the structure with the largest degree of bending of the DNA helix produced at the end of this simulation, i.e., the TA-DNA flanked by A-DNA (in *yellow*). Note that although both the A-DNA and TA-DNA component pieces of the structures shown in Fig. 5 are straight (Guzikevich et al., 1996), the bend observable in each of the full DNA structures results from the junction between different conformations, specifically from the different inclinations of the base pairs in A-DNA and TA-DNA (A/TA/A). The final TA-DNA conformation shown in Fig. 5 is the one attainable with a χ angle value corresponding to B-DNA (see *green broken line* in Fig. 1 *A*), in the context of a backbone structure corresponding to A-DNA (see *blue lines* in Fig. 1 *C*, and Table 2).

Fig. 5 also shows the average structure for the 8 bp of the TATA box computed from the trajectory between 200 and

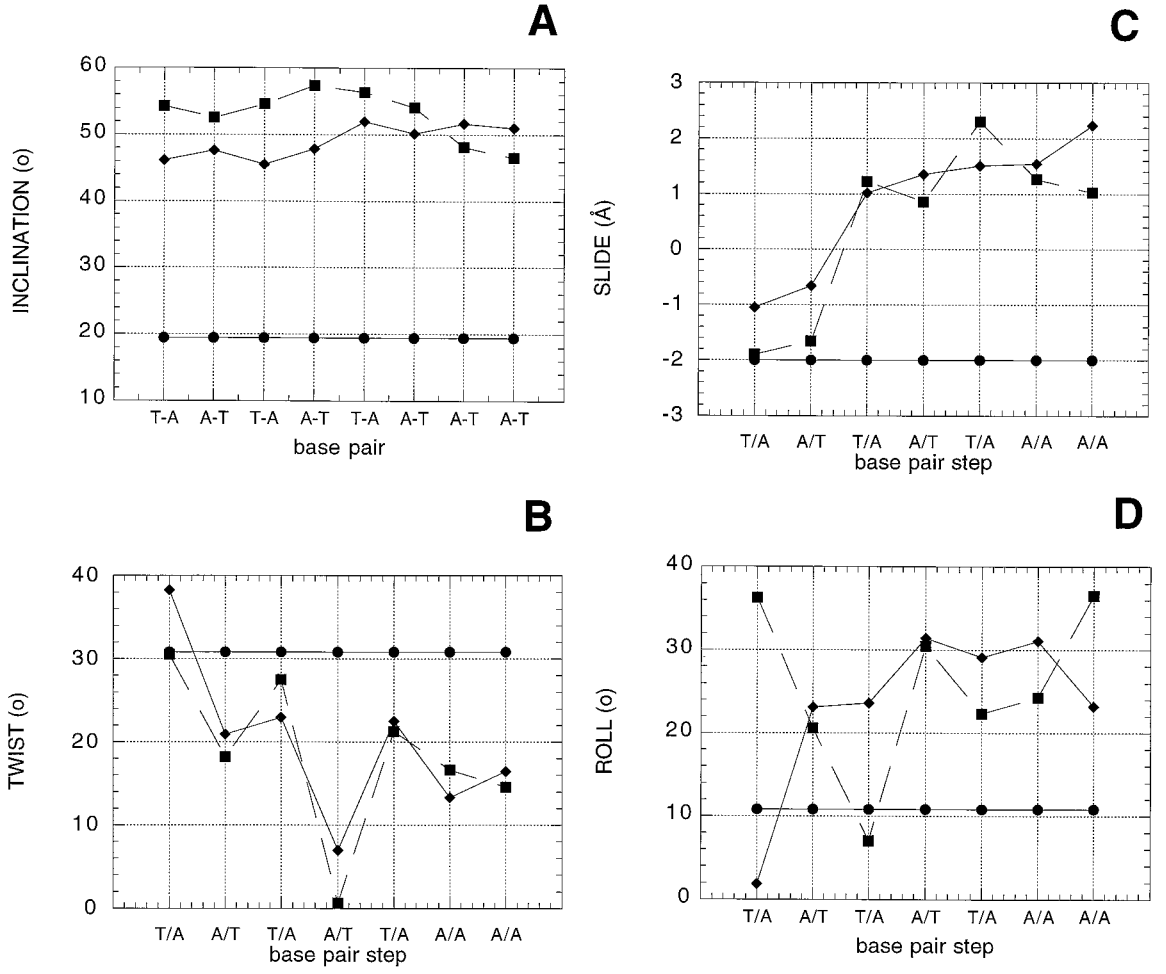

FIGURE 3 Comparison of base pair and base pair step geometrical parameters for the TATA box base pairs of A-DNA (●), a crystal structure of TA-DNA (Kim et al., 1993a) (■), and the average structure from the 200–250-ps interval of the simulation (◆). (*A*) Inclination; (*B*) twist; (*C*) slide; (*D*) roll. The structural parameters were calculated with CURVES as global parameters (Lavery and Sklenar, 1989), over the 8 bp of the TATA box. The *slide*, *roll*, and *twist* parameters were calculated with CURVES 4.1 (Lavery and Sklenar, 1989), whereas *inclination* was calculated with the CURVES version incorporated in the Dials and Windows package (Ravishanker et al., 1989).

250 ps, extended at the 5′ and 3′ ends by DNA in the B-DNA conformation (see *blue structure* and second part of Methods). Clearly, the bend observed in the various crystal structures (Geiger et al., 1996; Juo et al., 1996; Kim et al., 1993a,b; Kosa et al., 1997; Nikolov et al., 1995, 1996; Tan et al., 1996) results from the junction between the TA-DNA conformation in the TATA box and the B-DNA conformation at the boundaries of the TATA box (B/TA/B) (Lebrun et al., 1997).

The evolution of the structural rearrangement of DNA resulting from the gradual change in the value of the χ glycosyl bond angle throughout the constrained molecular dynamics simulation points to the possibility of finding many conformational intermediates on the path between the A-DNA and the TA-DNA conformations. Thus, following the hypothesis of Guzikevich et al. and assuming that the transition to a TA-DNA structure involves a transition from A-DNA, it is likely that DNA structures corresponding to some of these computational intermediates will be observed to exist independently when additional crystal structures of protein-DNA complexes of this kind become available.

CONCLUSIONS

It has recently been shown that unrestrained molecular dynamics simulations reproduce conformational transitions of the DNA molecule from A-DNA to B-DNA (Cheatham and Kollman, 1996) and from B-DNA to A-DNA (Yang and Pettitt, 1996), depending on the sequence, the force field used in the simulations, and the environmental conditions. From similar unrestrained molecular dynamics simulations of seven DNA dodecamers, we identified the sequence-dependent tendency for deformation related to TBP binding to TATA box sequences (Pastor et al., 1997a). It is important to note that a spontaneous transition to the TA-DNA conformation was not observed for any of these dodecamers. However, it appears that such studies reproduce the

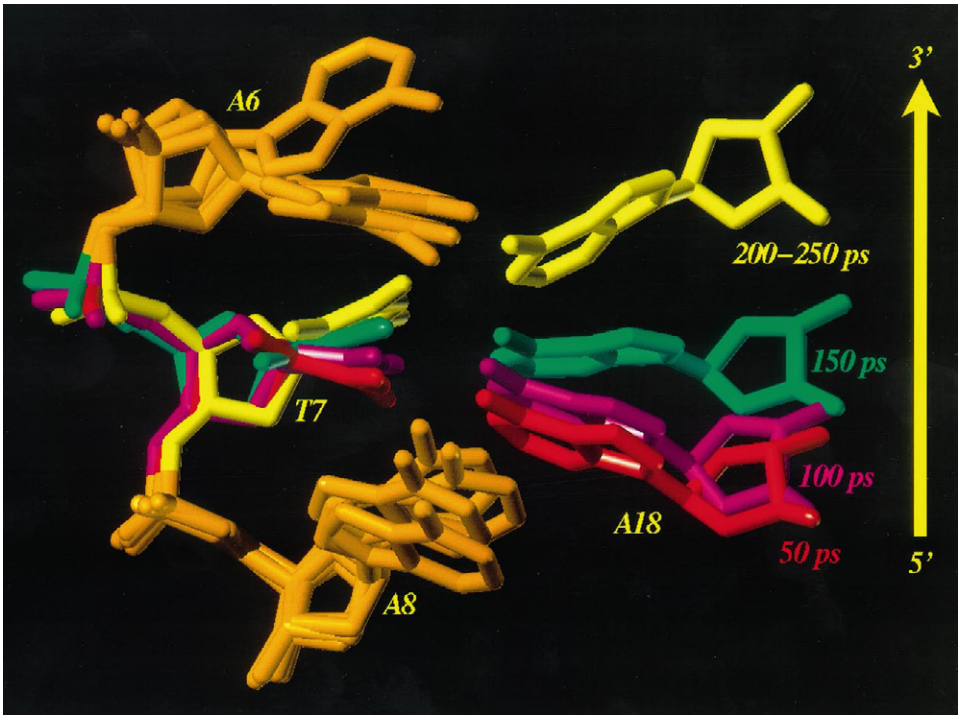

FIGURE 4 Structures of the central base pair T7:A18 of the TATA box at 50 ps (*red*), 100 ps (*purple*), 150 ps (*green*), and the average structure computed from the trajectory between 200 and 250 ps (*yellow*). The atoms of the backbones of A6, T7, and A8 were superimposed. This comparison emphasizes that the transition from A-DNA to TA-DNA, driven by the glycosyl-bond torsion angle, involves a continuous motion of the sugar moieties toward the 3′ end and a gradual change in the orientation of the base pair. The other base pairs of the TATA box behave in an identical manner.

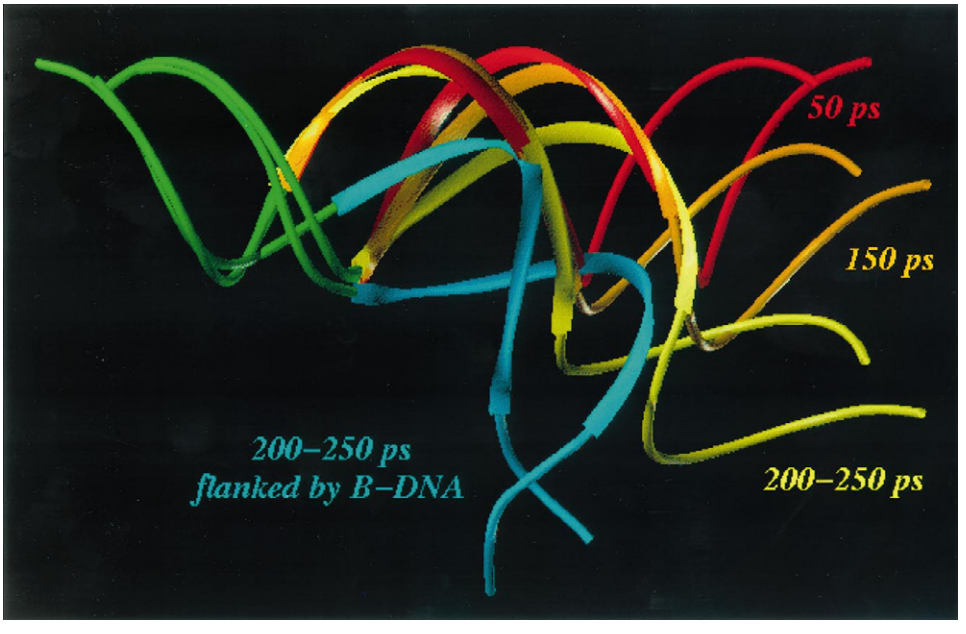

FIGURE 5 Structures from the A-DNA to TA-DNA conformational transition at 50 ps (*red*) and 150 ps (*orange*), and the average structure computed from the trajectory between 200 and 250 ps (*yellow and blue*). These TATA box structures have been extended at the 5′ and 3′ ends (see the second part of Methods, Progressive DNA Binding) by DNA segments in the A-DNA conformation (*red, orange, and yellow*) and B-DNA conformation (*blue*). The computed structures of the TATA box during the conformational transition are shown as flat ribbons, whereas the extensions are shown as tube ribbons. The structures were superimposed at the 5′ end extensions (in *green*).

apparent predisposition of DNA dodecamers containing TATA sequences toward attaining a conformation close to that of A-DNA (Pastor et al., 1997a; Pastor et al., 1997b; Flatters et al., 1997) that was observed experimentally (Shakked et al., 1983). Therefore, it is attractive to consider that the first step in the proposed mechanism of DNA bending involves the recognition of the TATA box in an A-DNA-like conformation, followed by an A-DNA to TA-DNA transition that could be achieved smoothly, as demonstrated here by modifying the value of the glycosyl-bond torsion angle, within the constraints of an A-DNA backbone.

Helpful suggestions of clarification and improvement by anonymous reviewers are gratefully acknowledged.

This work was supported in part by a grant from the Association for International Cancer Research (HW); grants from DGICYT, PB95-0624 and PR95-275 (LP); and a Fulbright/CONACyT scholarship (NP). Some of the simulations were run at the Cornell National Supercomputer Facility (sponsored by the National Science Foundation and IBM) and at the Centre de Computació i Comunicacions de Catalunya.

REFERENCES

Arnott, S., and D. W. L. Hukins. 1972. Optimized parameters for A-DNA and B-DNA. *Biochem. Biophys. Res. Commun.* 47:1504–1509.

Burley, S. K., and R. G. Roeder. 1996. Biochemistry and structural biology of transcription factor IID (TFIID). *Annu. Rev. Biochem.* 65:769–99.

Cheatham, T. E., III, and P. A. Kollman. 1996. Observation of the A-DNA to B-DNA transition during unrestrained molecular dynamics in aqueous solution. *J. Mol. Biol.* 259:434–444.

Choy, B., and M. R. Green. 1993. Eukaryotic activators function during multiple steps of preinitiation complex assembly. *Nature.* 366:531–536.

Cieplak, P., T. E. Cheatham, III, and P. A. Kollman. 1997. Molecular dynamics simulations find that 3′ phosphoramidate modified DNA duplexes undergo a B to A transition and normal DNA duplexes an A to B transition. *J. Am. Chem. Soc.* 119:6722–6730.

Cornell, W. D., P. Cieplak, C. I. Bayly, I. R. Gould, K. M. Merz, D. M. Ferguson, D. C. Spellmeyer, T. Fox, J. W. Caldwell, and P. A. Kollman. 1995. A second generation force field for the simulation of proteins, nucleic acids, and organic molecules. *J. Am. Chem. Soc.* 117: 5179–5197.

Darden, T. A., D. York, and L. Pedersen. 1993. Particle mesh Ewald: an *N* log(*N*) method for Ewald sums in large systems. *J. Chem. Phys.* 98: 10089–10092.

Elcock, A. H., and J. A. McCammon. 1996. The low dielectric interior of proteins is sufficient to cause major structural changes in DNA on association. *J. Am. Chem. Soc.* 118:3787–3788.

Flatters, D., M. Young, D. L. Beveridge, and R. Lavery. 1997. Conformational properties of the TATA-box binding sequence of DNA. *J. Biomol. Struct. Dyn.* 14:757–65.

Geiger, J. H., S. Hahn, S. Lee, and P. B. Sigler. 1996. Crystal structure of the yeast TFIIA/TBP/DNA complex. *Science.* 272:830–836.

Guzikevich Guerstein, G., and Z. Shakked. 1996. A novel form of the DNA double helix imposed on the TATA-box by the TATA-binding protein. *Nature Struct. Biol.* 3:32–37.

Juo, Z. S., T. K. Chiu, P. M. Leiberman, I. Baikalov, A. J. Berk, and R. E. Dickerson. 1996. How proteins recognize the TATA box. *J. Mol. Biol.* 261:239–254.

Kim, Y., J. H. Geiger, S. Hahn, and P. B. Sigler. 1993a. Crystal structure of a yeast TBP/TATA-box complex. *Nature.* 365:512–520.

Kim, J. L., D. B. Nikolov, and S. K. Burley. 1993b. Co-crystal structure of TBP recognizing the minor groove of a TATA element. *Nature.* 365: 520–527.

Kosa, P. F., G. Ghosh, B. S. DeDecker, and P. B. Sigler. 1997. The 2.1-Å crystal structure of an archaeal preinitiation complex: TATA-box-binding protein/transcription factor (II)B core/TATA-box. *Proc. Natl. Acad. Sci. USA.* 94:6042–6047.

Lavery, R., and H. Sklenar. 1989. Defining the structure of irregular nucleic acids: conventions and principles. *J. Biomol. Struct. Dyn.* 6:655–667.

Lebrun, A., and R. Lavery. 1997. Unusual DNA conformations. *Curr. Opin. Struct. Biol.* 7:348–354.

Lebrun, A., Z. Shakked, and R. Lavery. 1997. Local DNA stretching mimics the distortion caused by the TATA box-binding protein. *Proc. Natl. Acad. Sci. USA.* 94:2993–2998.

Nikolov, D. B., H. Chen, E. D. Halay, A. Hoffman, R. G. Roeder, and S. K. Burley. 1996. Crystal structure of a human TATA box-binding protein/TATA element complex. *Proc. Natl. Acad. Sci. USA.* 93:4862–4867.

Nikolov, D. B., H. Chen, E. D. Halay, A. A. Usheva, K. Hisatake, D. K. Lee, R. G. Roeder, and S. K. Burley. 1995. Crystal structure of a TFIIB-TBP-TATA-element ternary complex. *Nature.* 377:119–128.

Olson, W. K. 1977. Spatial configuration of ordered polynucleotide chains: a novel double helix. *Proc. Natl. Acad. Sci. USA.* 74:1775–1779.

Pastor, N., L. Pardo, and H. Weinstein. 1997a. Does TATA matter? A structural exploration of the selectivity determinants in its complexes with TBP. *Biophys. J.* 73:640–652.

Pastor, N., L. Pardo, and H. Weinstein. 1997b. How the TATA box selects its protein partner. *In* Molecular Modeling of Nucleic Acids. ACS Symp. Series No. 682. N. B. Leontis and J. Santa Lucia, editors. American Chemical Society, Washington DC. 329–345.

Pearlman, D. A., D. A. Case, J. W. Caldwell, W. S. Ross, T. E. Cheatham, D. M. Ferguson, G. L. Seibel, U. C. Singh, P. K. Weiner, and P. A. Kollman. 1995. AMBER, University of California, San Francisco.

Pugh, B. F. 1996. Mechanisms of transcription complex assembly. *Curr. Opin. Cell. Biol.* 8:303–311.

Ravishanker, G., S. Swaminathan, D. L. Beveridge, R. Lavery, and H. Sklenar. 1989. Conformational and helicoidal analysis of 30 ps of molecular dynamics on the d(CGCGAATTCCGCG) double helix: "Curves," Dials and Windows. *J. Biomol. Struct. Dyn.* 6:669–699.

Shakked, Z., D. Rabinovich, O. Kennard, W. B. Cruse, S. A. Salisbury, and M. A. Viswamitra. 1983. Sequence-dependent conformation of an A-DNA double helix. The crystal structure of the octamer d(G-G-T-A-T-A-C-C). *J. Mol. Biol.* 166:183–201.

Tan, S., Y. Hunziker, D. F. Sargent, and T. J. Richmond. 1996. Crystal structure of a yeast TFIIA/TBP/DNA complex. *Nature.* 381:127–134.

Yang, L., and B. M. Pettitt. 1996. B to A transition of DNA on the nanosecond time scale. *J. Phys. Chem.* 100:2564–2566.